Cancer Research

DFMO and 5-Azacytidine Increase M1 Macrophages in the Tumor Microenvironment of Murine Ovarian Cancer

Meghan Travers[1], Stephen M. Brown[1], Matthew Dunworth[1], Cassandra E. Holbert[1], Karla R. Wiehagen[2], Kurtis E. Bachman[2], Jackson R. Foley[1], Meredith L. Stone[1,3], Stephen B. Baylin[1], Robert A. Casero, Jr.[1], and Cynthia A. Zahnow[1]

Abstract

Although ovarian cancer has a low incidence rate, it remains the most deadly gynecologic malignancy. Previous work has demonstrated that the DNMTi 5-Azacytidine (5AZA-C) activates type I interferon signaling to increase IFNγ^+ T cells and natural killer (NK) cells and reduce the percentage of macrophages in the tumor microenvironment. To improve the efficacy of epigenetic therapy, we hypothesized that the addition of α-difluoromethylornithine (DFMO), an ornithine decarboxylase inhibitor, may further decrease immunosuppressive cell populations improving outcome. We tested this hypothesis in an immunocompetent mouse model for ovarian cancer and found that *in vivo*, 5AZA-C and DFMO, either alone or in combination, significantly increased survival, decreased tumor burden, and caused recruitment of activated (IFNγ^+) CD4$^+$ T cells, CD8$^+$ T cells, and NK cells. The combination therapy had a striking increase in survival when compared with single-agent treatment, despite a smaller difference in recruited lymphocytes. Instead, combination therapy led to a significant decrease in immunosuppressive cells such as M2 polarized macrophages and an increase in tumor-killing M1 macrophages. In this model, depletion of macrophages with a CSF1R-blocking antibody reduced the efficacy of 5AZA-C + DFMO treatment and resulted in fewer M1 macrophages in the tumor microenvironment. These observations suggest our novel combination therapy modifies macrophage polarization in the tumor microenvironment, recruiting M1 macrophages and prolonging survival.

Significance: Combined epigenetic and polyamine-reducing therapy stimulates M1 macrophage polarization in the tumor microenvironment of an ovarian cancer mouse model, resulting in decreased tumor burden and prolonged survival.

Introduction

Although ovarian cancer has a low incidence rate of 1.3% nationally, it remains the most deadly gynecologic malignancy and the need for novel therapeutics is high (1). Cancer immunotherapy treatment options have grown rapidly in the last decade and have demonstrated considerable promise in multiple disease types; however, ovarian tumors have thus far not responded well to current therapies such as the immune checkpoint inhibitors α-PD-1 and α-PD-L1 (2–5). Low intratumoral CD8$^+$ T cells and high immunosuppressive cell populations such as myeloid-derived suppressor cells (MDSC) and macrophages are associated with poor prognosis in ovarian cancer and could impact the efficacy of these immune therapies (6–9). Drug treatment strategies that alter the tumor and immune cell microenvironment could prolong survival for patients with ovarian cancer.

Macrophages demonstrate considerable plasticity in their development, responding to environmental signals such as cytokines and growth factors that dictate their phenotype (10). Classically polarized or M1 type macrophages are considered to be antitumorigenic, producing proinflammatory cytokines and promoting T-cell immunity (10–12). In contrast, alternatively polarized or M2 type macrophages, normally involved in wound repair, are anti-inflammatory and can promote tumorigenesis (10–12). In order for immune checkpoint blockades such as α-PD-1 to be effective, there must be a robust T-cell response in the tumor, and the relative proportions of these M1 and M2 macrophages has a significant impact on T-cell immunity (10).

One treatment strategy that impacts immune cell populations in the tumor microenvironment is epigenetic therapies such as DNA methyl transferase inhibitors (DNMTI) and histone deacetylase inhibitors (HDACI; refs. 13–19). 5-Azacytidine (5AZA-C) is a demethylating agent, which incorporates into nucleic acids as a cytidine analog that cannot be methylated by DNA methyl transferases (DNMT). 5AZA-C is FDA approved for myelodysplastic syndrome (MDS), and low nanomolar doses lead to decreased DNA promoter methylation and restored expression of

[1]Department of Oncology, The Sidney Kimmel Comprehensive Cancer Center at Johns Hopkins, Baltimore, Maryland. [2]Janssen Research & Development, Spring House, Pennsylvania. [3]Division of Hematology-Oncology, Department of Medicine, Perelman School of Medicine, University of Pennsylvania, Philadelphia, Pennsylvania.

Note: Supplementary data for this article are available at Cancer Research Online (http://cancerres.aacrjournals.org/).

Corresponding Authors: Cynthia A. Zahnow, Johns Hopkins University School of Medicine, 1650 Orleans Street, Baltimore, MD 21231. Phone: 410-955-2779; Fax: 410-614-9884; E-mail: zahnoci@jhmi.edu; and Robert A. Casero, Jr., rcasero@jhmi.edu

Cancer Res 2019;79:3445–54

doi: 10.1158/0008-5472.CAN-18-4018

hypermethylated genes in cancer (20). Additionally, 5AZA-C treatment induces the reexpression of hypermethylated, silenced endogenous retroviruses (ERV) *in vitro*, which can elicit an antiviral, interferon immune response that leads to T-cell activation *in vivo* (15, 18). Furthermore, 5AZA-C treatment of an ovarian cancer mouse model leads to increased immune cells in the tumor microenvironment, and combination 5AZA-C and HDACi sensitized tumors to α-PD-1 therapy (18). Although first-generation HDACIs combined with DNMTIs have demonstrated some promise in clinical trials for non–small cell lung cancer (21), there remains a need to discover novel treatment strategies that activate the immune system and provide long-term remission for other solid tumors.

Although the impact of epigenetic therapy on the immune system has been well established, emerging literature has shown that additional drug therapies can also regulate the immune system. In particular, polyamine-blocking therapy (PBT), the combined inhibition of polyamine biosynthesis and transport, significantly inhibits tumor growth in immunocompetent mice but not in athymic mice (22). Polyamines are naturally occurring, polycationic, alkyl amines that are absolute requirements for multiple cellular processes and are particularly important for tumor cell growth (23). 2-Difluoromethylornithine (DFMO) is FDA approved for African sleeping sickness, and works as an inhibitor of ornithine decarboxylase (ODC), an essential enzyme that catalyzes a rate-limiting step of polyamine synthesis. DFMO treatment reduces intracellular polyamines and inhibits tumor cell growth in multiple model systems, but failed to demonstrate significant antitumor activity as a single agent in advanced tumors (24–26). It is currently being tested in clinical trials as a chemopreventive agent and for the treatment of neuroblastoma (27–32).

Similar to data obtained with PBT, DFMO treatment alters immune cell populations in the tumor microenvironment (33). Investigators demonstrated that DFMO treatment of immunocompetent mice, but not RAG1 knockout mice, inhibited tumor growth, decreased MDSC activity, and increased infiltration of $CD8^+$ T cells (33). The potential to combine epigenetic therapy with PBT is intriguing, as epigenetic therapies are known to activate a strong antiviral, interferon response, whereas PBT attenuates immunosuppressive cells such as MDSCs.

We have therefore tested the hypothesis that the combination of 5AZA-C and DFMO would produce a more durable antitumor response due to immune-related changes in the tumor microenvironment. In an immunosuppressive mouse model of aggressive high-grade serous ovarian cancer, we found that combination 5AZA-C and DFMO dramatically prolonged survival, and led to an increase in M1 versus M2 macrophages that may be important for the efficacy of this drug combination. Because both drugs are clinically approved and well-tolerated, there is potential to rapidly translate this combination to the clinic for treatment of ovarian cancer. Moreover, other solid tumors that are rich in macrophages could benefit from this treatment regimen as well, due to the impact this drug combination has on macrophage polarization.

Materials and Methods

Drugs and reagents

DFMO was kindly provided by Dr. Patrick Woster (Medical University of South Carolina, Charleston, SC). 5AZA-C was purchased from Sigma-Aldrich (Catalog No. 320-67-2). α-PD-1 was kindly provided by the Michael Lim lab. α-CSF1R (BioXCell Clone AFS98) was generously provided by Janssen.

Animals

Female C57BL/6NHsd wild-type (WT) mice (7- to 8-week-old) were purchased from Envigo International Holdings, Inc. Mice were housed at the Johns Hopkins Kimmel Cancer Center Animal Resources Core and cared for in accordance with the policies of The Johns Hopkins University Animal Care and Use Committee and our approved animal protocol.

Syngeneic mouse model

A total of 250,000 VEGF-β-Defensin ID8 (VDID8) syngeneic mouse ovarian surface epithelial (MOSE) cells were injected intraperitoneally into wild-type (WT) C57BL/6 mice. Cells were obtained from Dr. Chien-Fu Hung and tested for *Mycoplasma* every 6 months using MycoAlert PLUS (Lonza; LT07-701) per manufacturer's instructions and as previously described (18). Dr. Katherine Roby developed the ID8 model via mild trypsinization of the ovarian surface epithelium, followed by long-term passage *in vitro* until the cells spontaneously immortalized (34). The parental ID8 clone has been further modified to enhance its usefulness as a tool by overexpressing VEGF and β-defensin, making the tumor more aggressive and immunosuppressive (35). The VDID8 cells are also positive for luciferase and GFP. Although this model has proven to be an excellent research tool, it has limitations in representing high-grade serous ovarian cancer in humans because it is derived from mouse ovarian surface epithelium, not the fallopian tube, and is Trp53 WT. In mice however, ovarian cancer can arise from either fallopian tube epithelium (FTE) or ovarian surface epithelium (OSE) and ID8 is the most widely used MOSE model for immunotherapy studies in ovarian cancer.

Mice were treated with 0.5 mg/kg 5AZA-C/saline, Monday to Friday, every other week and continuous 2% DFMO in drinking water. Two hundred micrograms of α-PD-1 or IgG was injected intraperitoneally four times total on days 17, 20, 24, and 27 after intraperitoneal injection of VDID8 cells. Two hundred micrograms of α-CSF1R or IgG was injected intraperitoneally twice weekly beginning 2 weeks prior to VDID8 cell injection, and continuing throughout the duration of the experiment.

Ascites tissue harvest and processing

When ascites fluid is collected from the mice, the cells obtained represent the tumor microenvironment and can be further analyzed to help illustrate the mixed population of cells surrounding the tumor. Ascites was collected, filtered, incubated in ACK buffer (Quality Biological) to lyse red blood cells, and washed. The mononuclear cells collected were then cultured for 4 hours in RPMI (Corning) with 10% FBS in the presence of phorbol 12-myristate 13-acetate (PMA) and ionomycin to stimulate cells, and brefeldin A and monensin (Invitrogen; 00-4975-93) to cause aggregation of secreted proteins inside the cell.

Flow cytometry

Cells were washed and blocked with FcR Blocking Reagent (Miltenyi Biotec; 130-092-575) and stained for cell-surface markers including Live/Dead (eBioscience; 65-0865-14), CD45 (BD Biosciences; 563891), CD3 (BD Biosciences; 560527), CD4 (BD Biosciences; 563331), CD8 (BD Biosciences; 563152), NK1.1 (BD Biosciences; 562921), F4/80 (BioLegend; 123113), CD11b

(BioLegend; 101222), MHC II (isotype control; 400627; BioLegend; 107619), CD206 (BioLegend; 141708), CD11c (BD Biosciences; 564079), Ly6C (BD Biosciences; 562728), Ly6G (BD Biosciences; 563005), CD80 (BD Biosciences; 553769), and CD86 (BD Biosciences; 558703). Cells were permeabilized and stained for intracellular IFNγ (isotype control 554686; BD Biosciences; 554413). Flow cytometry acquisition was performed on an LSR II cytometer (BD Biosciences), and data were analyzed using FlowJo software version 10.2.

Flow sorting

Lysed and processed bulk ascites cells were blocked with FcR Blocking Reagent (Miltenyi Biotec; 130-092-575) and stained for cell-surface markers including Live/Dead (eBioscience; 65-0865-14), CD45 (BD Biosciences; 563891), F4/80 (BioLegend; 123113), CD11b (BioLegend; 101222), MHC II (isotype control; 400627; BioLegend; 107619), CD206 (BioLegend; 141708), and CD11c (BD Biosciences; 564079). Prepared cells were suspended in PBS and sorted immediately on a BSL-2 FACSAria II. M1 macrophages were sorted on a gate as follows: $CD45^+$ L/D^- F4\80$^+$ $CD11b^+$ MHC II^+ $CD206^-$ $CD11c^-$. M2 macrophages were sorted on a gate as follows: $CD45^+$ L/D^- F4\80$^+$ $CD11b^+$ MHC II^- $CD206^+$ $CD11c^-$.

RNA isolation and quantitative reverse-transcriptase PCR

Total RNA was isolated from sorted macrophages using TRIzol reagent according to the manufacturer's protocol (Invitrogen). Two hundred nanograms of RNA were used for cDNA synthesis using qScript cDNA SuperMix (Quanta Biosciences), followed by SYBR green-mediated real-time PCR (Universal SYBR Green Supermix; Bio-Rad) using custom primers specific for Arg1, Fizz1, and iNOS2 (Arg1 F: CAGAAGAATGGAAGAGTCAG; Arg1 R: CAGATATGCAGGCAGGGAGTCACC; Fizz1 F: GGTCCCAGTG-CATATGGATGAGACCA; Fizz1 R: CACCTCTTCACTCGAGGGA-CAGTTGG; iNOS2 F: CCGAAGCAAACATCACATTCA; iNOS2 R: GGTCTAAAGGCTCCGGGCT). In each experiment, samples were performed in duplicate, normalized to β-actin as an internal control, and fold change in expression relative to M1 or M2 macrophage was determined using the $2-\Delta\Delta C_t$ algorithm. Thermocycling was performed on a Bio-Rad iQ2 real-time PCR detection system and data collected using the iQ5 optical system software.

ELISA assays

Bulk ascites fluid collected from individual treated mice was centrifuged at low speed (1,000 rpm) for 15 minutes, and 1,000 μL of supernatant was collected and stored at −80°C. Circulating CSF1 levels in mice treated with IgG versus CSF1R was detected using an ELISA Kit (R&D Systems Kit #MMC00) according to instructions.

Polyamines

Polyamines were analyzed via high-performance liquid chromatography (HPLC) as previously described (36).

Statistical analysis

Data were graphed in GraphPad Prism 7.0 and tested for a Gaussian distribution using the Shapiro–Wilk test. Significance was determined for sets of data with more than 2 groups using the one-way ANOVA or Kruskal–Wallis test dependent upon normality results from the Shapiro–Wilk test. If only 2 sets of data were compared, either the Mann–Whitney (nonparametric) or Student *t* test (parametric) were used dependent on normality results. Significances in survival data were determined by Mantel–Cox (log-rank) test. *P* values less than 0.05 were deemed significant. Outliers were removed from ascites volume datasets and ascites immune cell datasets using Peirce criterion (37). Significances are shown as *, $P < 0.05$; **, $P < 0.01$; ***, $P < 0.001$; ****, $P < 0.0001$.

Results

Combination 5AZA-C and DFMO therapy reduces tumor burden and increases survival in an ovarian cancer mouse model

To confirm that DFMO inhibits ODC in the model systems used, VDID8 cells were treated *in vitro* and *in vivo* and polyamine levels were determined (Supplementary Fig. S1A and S1B). *In vitro* treatment of VDID8 tumor cells led to a significant decrease in putrescine and spermidine with DFMO alone and when combined with 5AZA-C. However, 5AZA-C alone appeared to have a stimulatory effect on putrescine and spermidine synthesis (Supplementary Fig. S1A). In bulk ascites cells from treated animals, combination treatment led to a decrease in all 3 polyamines, including spermine (Supplementary Fig. S1B). No significant changes to the polyamine pools were observed with 5AZA-C treatment alone, but putrescine and spermidine were decreased (although not significantly) by DFMO treatment (Supplementary Fig. S1B).

To test the hypothesis that addition of DFMO to therapy using the DNMTi 5AZA-C would reduce tumor burden and improve overall survival in a mouse model of ovarian cancer, immunocompetent C57BL/6 mice were injected intraperitoneally with 250,000 VDID8 syngeneic MOSE cells. Mice were treated intraperitoneally with 5AZA-C (0.5 mg/kg) or saline vehicle, DFMO (2% in water), or combination 5AZA-C and DFMO beginning 3 days posttumor injection (Fig. 1A). Hemorrhagic ascites fluid consistently develops at approximately 4 to 5 weeks after VDID8 injection and is an accurate measurement of tumor burden in mice, allowing observation of tumor growth in real time (35, 38). After draining hemorrhagic ascites fluid from mice for the second time (typically week 5 posttumor injection), mice treated with single-agent 5AZA-C or DFMO present with higher tumor burden than mice treated with combination therapy (Fig. 1B). Mice treated with combination therapy also exhibited the largest increase in overall survival with a median survival of 59 days compared with that of single-agent 5AZA-C or DFMO of approximately 44 days (Fig. 1C). Although total numbers of lymphocytes are significantly increased by single-agent 5AZA-C or DFMO compared with vehicle, these numbers are not further enhanced with combination 5AZA-C + DFMO treatment (Fig. 1D and E).

5AZA-C and DFMO combination treatment significantly increases IFNγ$^+$ natural killer cells

To pursue further whether changes in lymphocyte populations might account for the dramatic increase in survival observed with 5AZA-C + DFMO combination therapy, the numbers and activity of specific lymphocyte subpopulations in hemorrhagic ascites fluid at week 5 posttumor injection were analyzed. Single-agent 5AZA-C or DFMO led to significant increases in T-cell, natural killer (NK)-cell, and IFNγ$^+$ lymphocyte populations examined in

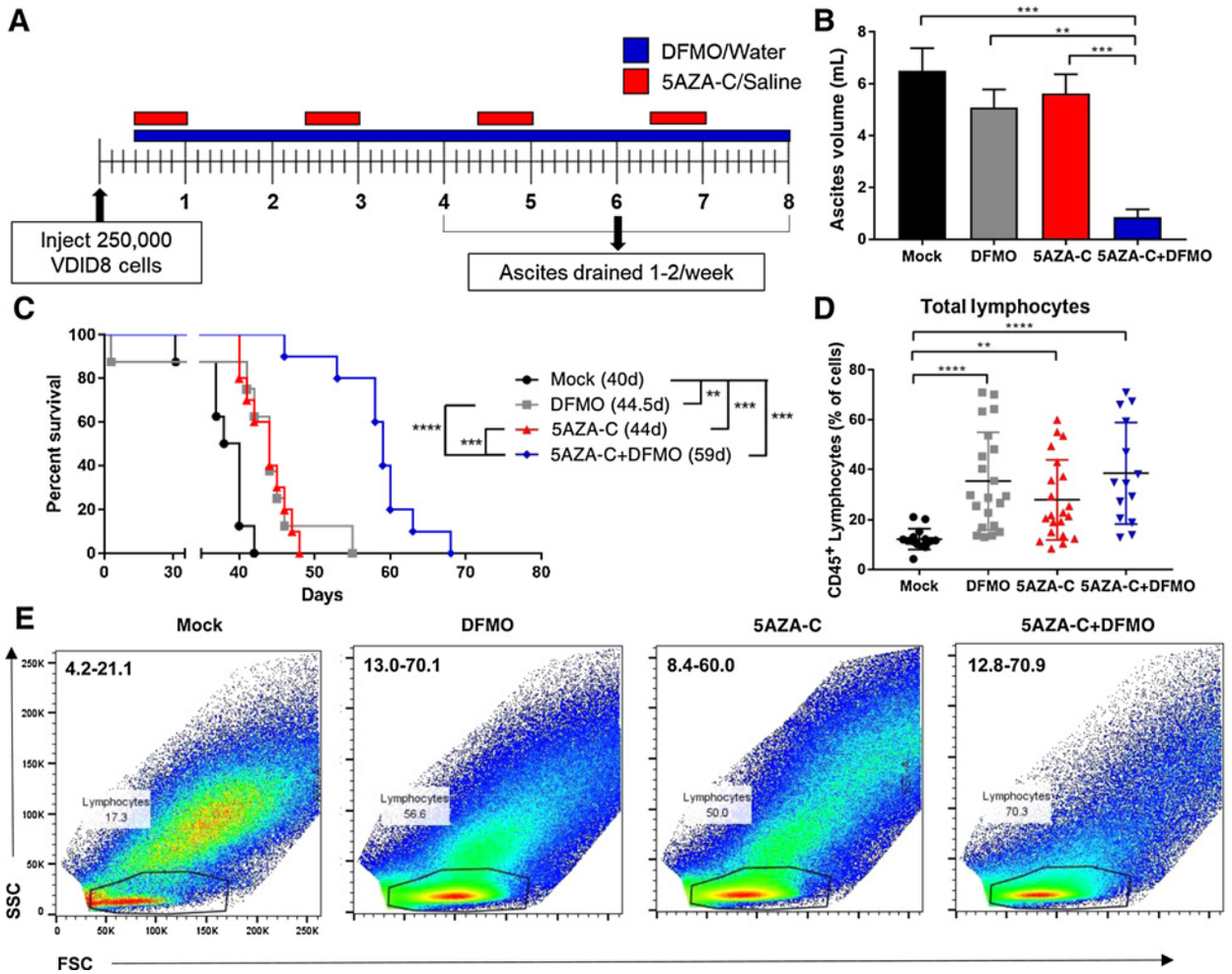

Figure 1.

Combination 5AZA-C + DFMO reduces tumor burden and increases survival in an ovarian cancer mouse model. **A,** Tumor cell injection and treatment schematic. Mice were injected intraperitoneally with 250,000 VEGF-DEFB ID8 MOSE cells (VDID8). 0.5 mg/kg of 5AZA-C was given intraperitoneally 5 days a week, every other week. Two percent of DFMO was provided in water bottles. Mice were treated throughout the duration of the experiment. Upon 25% to 30% weight gain, ascites fluid was drained from mice and processed for analysis of the tumor microenvironment. **B,** Tumor burden, represented by ascites volume, 5 weeks posttumor injection. Data are from the second ascites drain procedure; the first was 4 weeks posttumor injection. Representative data (mean ± SEM shown, $n = 10$; 4 biological replicates). Data were tested for a Gaussian distribution using Shapiro–Wilk test and found not to be normal. Significance was determined using Kruskal–Wallis test; statistical outliers removed using Peirce criterion. **C,** Representative survival curve (median survival in days; $n = 10$; 4 biological replicates). Significance determined using log-rank Mantel–Cox test. **D,** Total lymphocyte populations in bulk ascites fluid of mice at week 5 bulk; $n = 14$–21. Data were tested for a Gaussian distribution using Shapiro–Wilk test and found to be normal after log transformation. Significance was determined using one-way ANOVA. **E,** Flow cytometry plots of SSC versus FSC, demonstrating an increase in lymphocyte populations in ascites fluid at week 5 posttumor injection with 5AZA-C, DFMO, and 5AZA-C+DFMO treatment. Range of total lymphocyte population percentages are included in the top left-hand corner for each plot. **, $P < 0.01$; ***, $P < 0.001$; ****, $P < 0.0001$.

the tumor microenvironment (Fig. 2A–G). In most cases, combination therapy did not alter immune populations over what was observed with single agents (Fig. 2A–F). The exception, however, was a significant increase in IFNγ$^+$ NK cells observed in combination-treated mice versus 5AZA-C or DFMO alone (Fig. 2G). It was hypothesized that the observed increase in IFNγ$^+$ cells in the model could lead to an increase in PD-L1 expression on the surface of tumor cells, possibly sensitizing the tumor to α-PD-1 therapy. Surface PD-1 expression on T cells is a signature of immune tolerance, and when engaged with its ligand PD-L1 on tumor cells, can limit the T cell's ability to proliferate and perform its effector functions (39, 40). Addition of α-PD-1 to the combination of DFMO and 5AZA-C treatment did not further decrease tumor burden in the mice, nor did it increase survival (Supplementary Fig. S2A–S2F). No changes were observed in the number of PD-1 expressing cells with single-agent or combination treatment on either CD4$^+$ or CD8$^+$ T cells (Supplementary Fig. S2G and S2H). The lack of response to α-PD-1 therapy suggests that a T-cell response may not be the primary mechanism of action in this combination drug therapy. Although 5AZA-C and DFMO treatment led to elevated IFNγ$^+$ NK cells and modest increases in T cells, it does not appear that the differences between

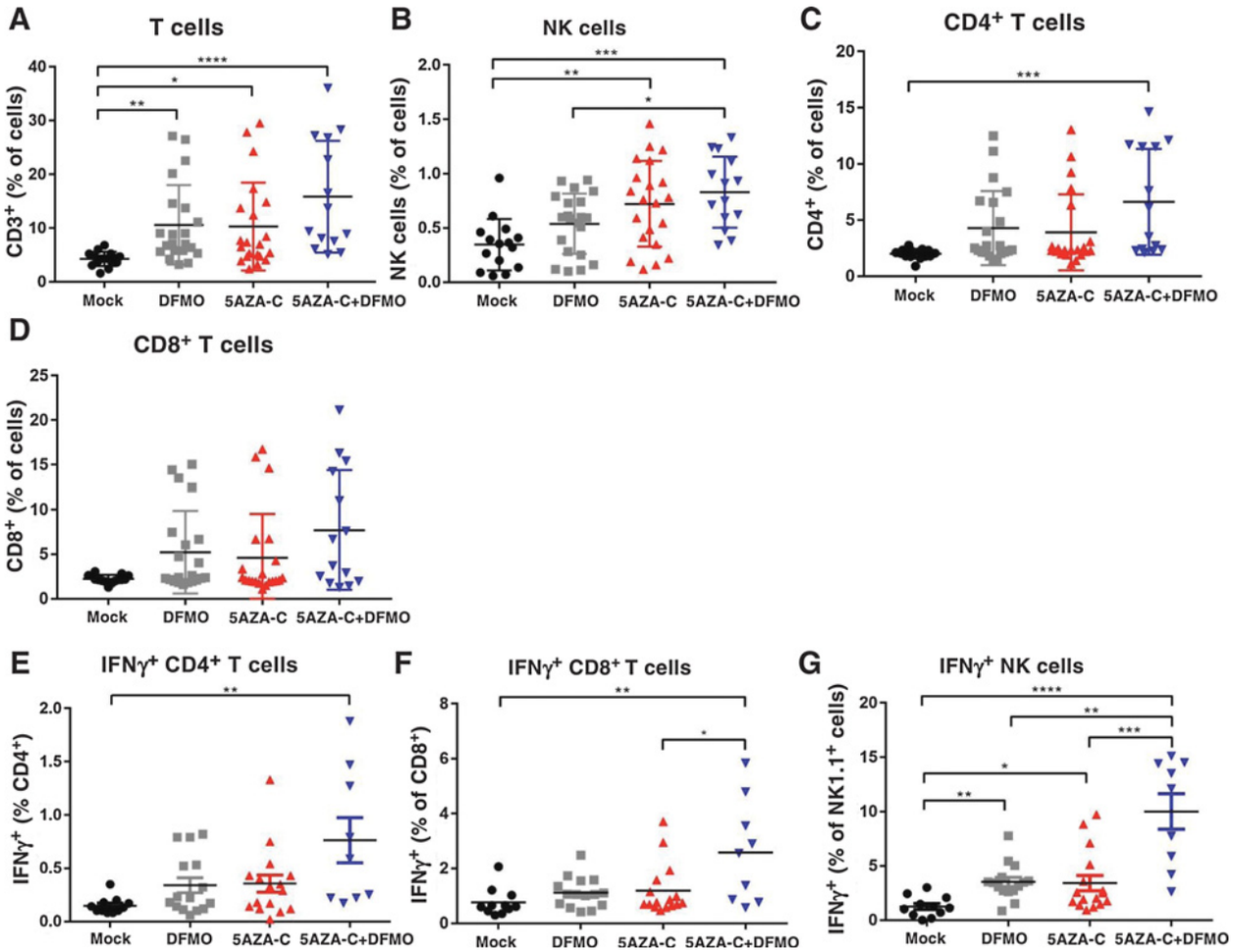

Figure 2.

Combination 5AZA-C + DFMO elevates lymphocyte populations and IFNγ$^+$ lymphocytes in tumor associated ascites. Ascites fluid was collected from treated mice and the cellular fraction was processed for FACS analysis. FACs analysis of cellular populations isolated from ascites at week 5 post-injection demonstrates that combination treatment of 0.5 mg/kg 5AZA-C and 2% DFMO was the most effective at significantly elevating total T cells (**A**), NK cells (**B**), and CD4$^+$ T cells (**C**). An upward trend in total CD8$^+$ T cells (**D**) was observed as well. Both CD4$^+$ and CD8$^+$ T cells (**E** and **F**) and NK cells (**G**) showed an increase in IFNγ$^+$ cells with combination treatment. IFNγ$^+$ NK cells were significantly increased with combination 5AZA-C + DFMO compared with both single agent 5AZA-C or DFMO alone. Each data point represents cells harvested from one mouse; $n = 14–21$. All data were tested for a Gaussian distribution using Shapiro–Wilk test. Significance was determined using one-way ANOVA (**A**, **B**, and **E–G**) or Kruskal–Wallis test (**C** and **D**), dependent upon normality results from Shapiro–Wilk test. *, $P < 0.05$; **, $P < 0.01$; ***, $P < 0.001$; ****, $P < 0.0001$.

combination treatment and single agents 5AZA-C or DFMO were significant enough to explain the dramatic increase in survival seen with combination treatment (Fig. 1C).

Combination 5AZA-C + DFMO treatment results in a significant decrease in macrophages

The myeloid immune cell populations were next examined to determine whether a decrease in immunosuppression may account for the striking differences in survival. MDSCs are suppressive immune cells sometimes present in the tumor microenvironment, high levels of which are associated with a poor prognosis in ovarian cancer (7). No significant decrease in nonlymphocyte or MDSC populations was observed after treatment with 5AZA-C and DFMO (Fig. 3A and B). Instead, total macrophage populations in the tumor microenvironment were consistently decreased with 5AZA-C treatment, and decreased even further with the addition of DFMO (Fig. 3C). Macrophages are professional antigen-presenting cells capable of activating T cells. Surface expression of MHC II is essential for interaction with T cells, and the number of MHC II positive cells was increased with 5AZA-C, DFMO, and 5AZA-C + DFMO treatment compared with vehicle (Fig. 3D and E; Supplementary Fig. S3A and S3B). Importantly, MHC II expressing cells were increased significantly with combination treatment compared with single-agent 5AZA-C, suggesting a possible explanation for the dramatic increase in survival (Figs. 1C and 3D). In contrast, untreated mice had high populations of macrophages negative for the MHC II surface protein. These data suggest that macrophages may play an important role in tumor response to the combination drug therapy.

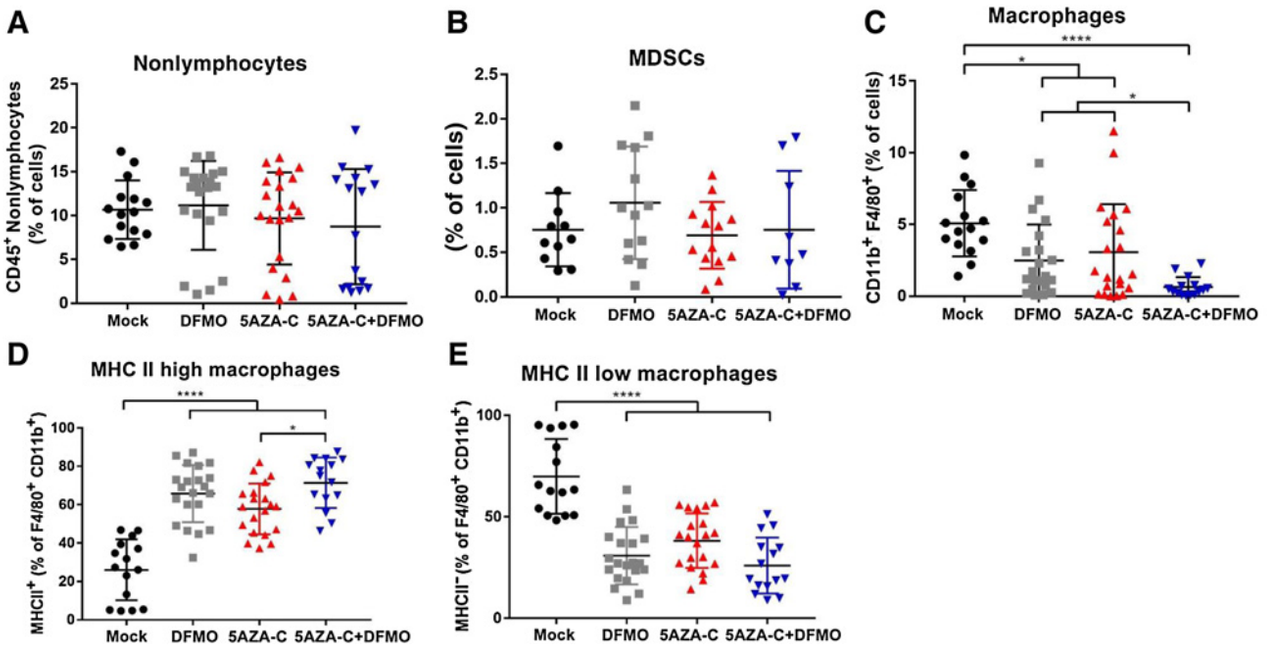

Figure 3.

5AZA-C + DFMO combination therapy decreases macrophages and alters the ratio of MHC II high to MHC II low macrophages. Ascites fluid was collected from treated mice and the cellular fraction was processed for FACS analysis. No changes were observed between any of the treatment arms for nonlymphocytes (**A**) or MDSCs (**B**). A significant decrease in total macrophages was observed in combination-treated mice compared with vehicle, as well as a significant decrease compared with 5AZA-C alone (**C**). Further analysis of macrophage populations revealed that the MHCII low (M2-like) population was decreased in all treatment arms (**D**), whereas the MHCII Hi (M1-like) population was increased across treatment arms (**E**). All data were tested for a Gaussian distribution using Shapiro–Wilk test. Significance was determined using one-way ANOVA (**B**–**E**) or Kruskal–Wallis test (**A**), dependent upon normality results from Shapiro–Wilk test. *, $P < 0.05$; ****, $P < 0.0001$.

Combination 5AZA-C + DFMO treatment leads to an increased ratio of M1 macrophages to M2 macrophages in the tumor microenvironment

Next, surface markers were examined to distinguish between classical (M1) and alternative (M2) polarized macrophages. High populations of M2 macrophages are associated with a poor prognosis due to their ability to promote tumor growth (8–10). Because the surface marker CD206 is upregulated on M2 macrophages, flow cytometry was used to analyze macrophages high for CD206 and low for MHC II—a surface marker for M1 macrophages. Although total macrophages were decreased by the treatments, an increase in M1 macrophages was observed in the remaining macrophage population for all treatment groups (Fig. 4A), as well as a decrease in M2 macrophages (Fig. 4B; Supplementary Fig. S4A). MHC II^- $CD206^+$ and MHC II^+ $CD206^-$ macrophages were then sorted via flow cytometry, and RNA was isolated to perform RT-PCR on M1- and M2-specific genes (41–44). As expected, $CD206^+$ macrophages demonstrated increased expression of Arg1 and Fizz1 compared with $CD206^-$ macrophages (Fig. 4C and D), and MHC II^+ macrophages had increased expression of iNOS2 compared with MHC II^- macrophages (Fig. 4E). These data confirm that macrophages expressing high levels of CD206 in our model also retain gene expression patterns that are characteristic of alternatively polarized M2 macrophages.

Interestingly, the decrease in M2 macrophages observed in 5AZA-C + DFMO-treated mice was not a durable response, and as tumor burden increased in these mice, the relative proportion of M2 macrophages increased as well (Supplementary Fig. S5A and S5B). Macrophages in vehicle-treated mice were therefore assessed at 3 different time points to determine whether M2 macrophages increase as the disease progresses. Indeed, relative levels of M2 macrophages increased as tumor burden increased in these mice, suggesting the importance of macrophages in disease progression of this ovarian cancer model (Fig. 4f).

Blocking macrophages with CSF1R antibody diminishes the 5AZA-C + DFMO response in the ovarian cancer mouse model

To test whether the increase in M1 macrophages was important in the response to 5AZA-C and DFMO treatment, macrophages were blocked in the ovarian cancer mouse model using an antibody to CSF1R (Fig. 5A; ref. 45). Treatment with α-CSF1R resulted in decreased macrophages in the tumor microenvironment (Fig. 5B) and a consequential increase in M-CSF levels in ascites fluid as measured by ELISA (Fig. 5C). Increased M-CSF indicates that the α-CSF1 receptor block antibody is functional, as more ligand (M-CSF) is free, and less ligand is engaged with its receptor (45). Initially, the 5AZA-C + DFMO combination treatment still resulted in decreased tumor burden in mice, even with the observed decrease in macrophages; however, over time, tumor burden increased more rapidly in 5AZA-C + DFMO mice receiving α-CSF1R (Fig. 5D and E). This decrease in macrophages also led to a decrease in overall survival, compared with 5AZA-C + DFMO mice that received IgG control (Fig. 5F). Analysis via flow cytometry of M1 and M2 surface markers showed that with IgG control, 5AZA-C + DFMO mice had increased M1 macrophages and decreased M2 macrophages compared with vehicle, as was previously seen (Figs. 5G and H and 4A

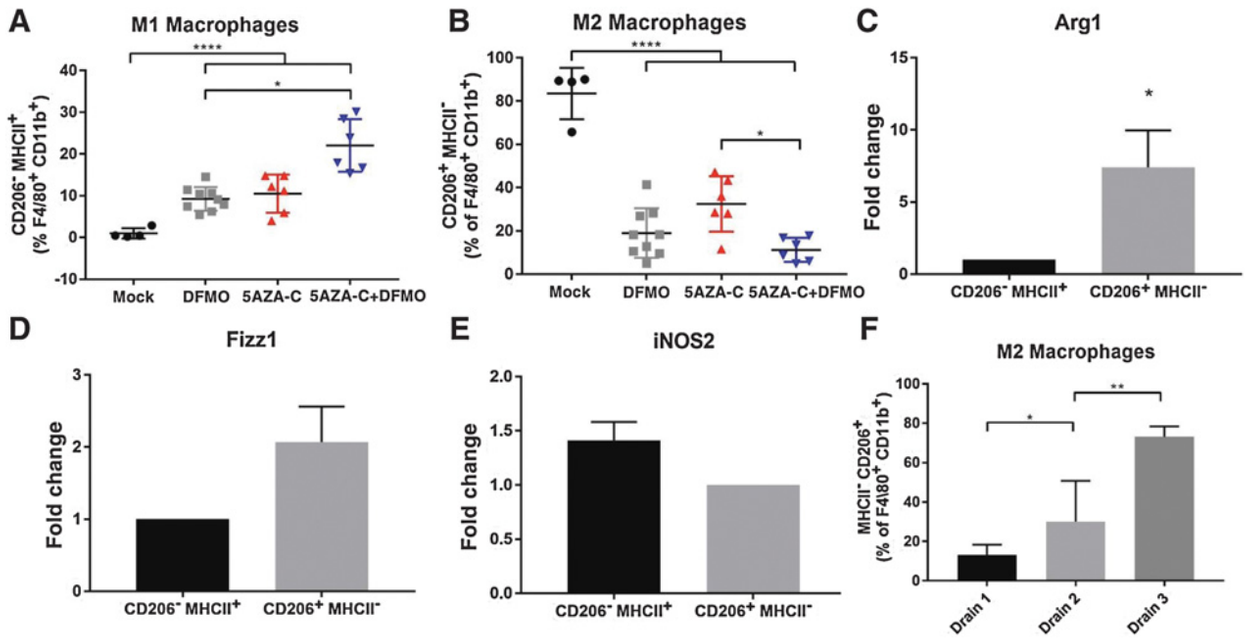

Figure 4.

5AZA-C + DFMO treatment reduces M2 polarization and increases M1 polarized macrophages in the tumor microenvironment. **A,** Percentage of M1 macrophages (MHC II$^+$ CD206$^-$) were increased with DFMO and 5AZA-C treatment, and further increased with combination 5AZA-C + DFMO treatment. **B,** Percentage of M2 macrophages (MHC II$^-$ CD206$^+$) was reduced in all treatment arms, with the greatest reduction observed in combination 5AZA-C + DFMO treatment. Macrophages were sorted from bulk ascites fluid collected from mice at week 5 posttumor injection. qRT-PCR for Arg1 (**C**) and Fizz1 (**D**) was performed on sorted macrophages (M2 macrophages = CD45$^+$ L/D$^-$ F4\80$^+$ CD11b$^+$ MHC II$^-$ CD206$^+$; M1 macrophages = CD45$^+$ L/D$^-$ F4\80$^+$ CD11b$^+$ MHC II$^+$ CD206$^-$). Data confirm that MHC II$^-$ CD206$^+$ macrophages exhibited gene expression signatures typical of M2 polarization. **E,** qRT-PCR of iNOS2 in M1 macrophages vs. M2 macrophages confirming that MHC II$^+$ CD206$^-$ macrophages exhibited gene expression signatures typical of M1 polarization. **F,** Percentage of M2 macrophages (MHCII$^-$ CD206$^+$) increase with tumor burden in vehicle-treated mice. Drain 1 was performed at week 4 posttumor cell injection; drain 2 at week 5 and drain 3 at week 6. All data were tested for a Gaussian distribution and found to be normal using Shapiro–Wilk test. Significance was determined using one-way ANOVA (**A** and **B**) or *t* test (**C–E**). *, $P < 0.05$; **, $P < 0.01$; ****, $P < 0.0001$.

and B). Interestingly, although 5AZA-C + DFMO mice maintained low M2 macrophages in the presence of α-CSF1R (consistent with the action of α-CSF1R; Fig. 5B), M1 macrophages were significantly decreased compared with 5AZA-C + DFMO mice receiving IgG control (Fig. 5G and H). These results indicate that the presence of M1 macrophages is important for the mechanism of action of this combination drug therapy, as 5AZA-C + DFMO-treated mice receiving α-CSF1R had decreased survival and increased tumor burden compared with IgG control.

Discussion

Combination epigenetic and polyamine reducing therapy is an effective treatment strategy for ovarian cancer in immunocompetent mice, prolonging survival and decreasing tumor burden significantly. This treatment regimen represents the first combination of these two drug therapies in mice, and the first use of DFMO in an immunocompetent mouse model for ovarian cancer (46). Treatment with 5AZA-C alone led to an increase in IFNγ$^+$ NK cells, CD4$^+$ T cells, and CD8$^+$ T cells, as has been demonstrated before (14, 18, 19). Signaling of IFNγ via its receptor IFNGR1 on tumor cells can lead to increased expression of PD-L1 on tumor cells, thereby making this increase in IFNγ an attractive candidate for α-PD-1 therapy. However, α-PD-1 therapy had no significant impact on survival in this model when added to the combination 5AZA-C and DFMO. These results are in contrast to previous studies using 5AZA-C and HDACi where the addition of α-PD-1 produced a significant therapeutic response (18). Histone acetylation is essential for transcription of IFNγ, therefore the use of an HDACi may explain the sensitization to α-PD-1 therapy previously seen, as increasing histone acetylation even further increased IFNγ levels in lymphocytes (47).

Analysis of the tumor microenvironment after the combination treatment with 5AZA-C and DFMO indicated that the impacts on macrophage polarization are critically important in this model. 5AZA-C treatment has been shown to decrease macrophages in the tumor microenvironment, although previously no distinction was made as to the polarization status of these macrophages (18, 19). As the understanding of macrophages deepens, research has discovered that these cells once thought of as permanent, differentiated cells, are in fact quite plastic and able to respond to multiple signals including cytokines and chemokines that direct their behavior and alter their phenotype. Classically polarized M1 macrophages, induced by cytokines such as IFNγ and IL12, upregulate expression of MHC II and can have tumoricidal functions. M1 macrophages metabolize arginine via iNOS to nitric oxide (NO), creating an oxidizing environment that is damaging to surrounding cells. DFMO treatment has been found to potentiate NO production in LPS-stimulated macrophages *in vitro* (48). In addition, DFMO, via product inhibition through the increase in ODC substrate, ornithine, inhibits the enzyme arginase I, which is essential for function of alternatively polarized M2

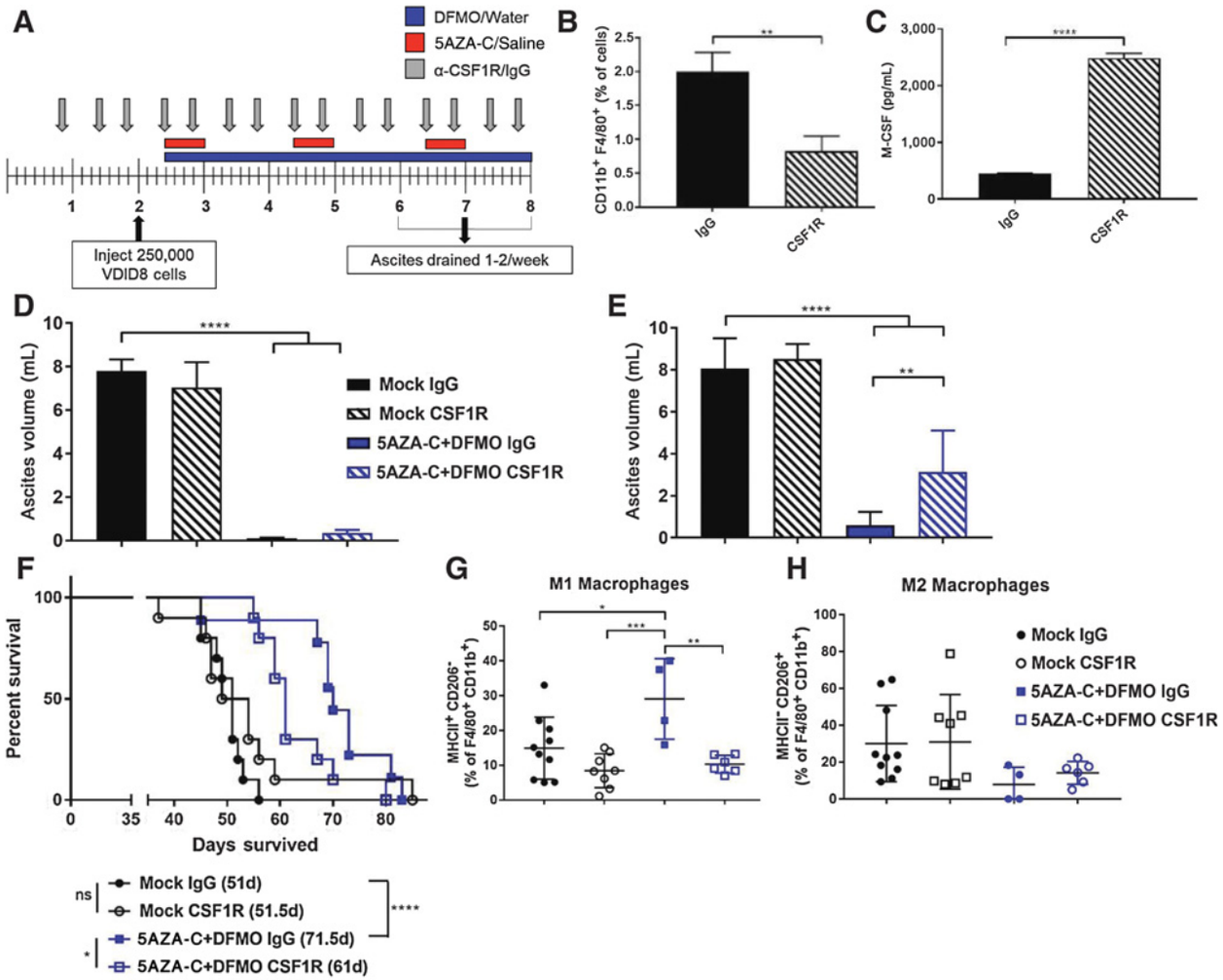

Figure 5.

Increased M1 macrophages are essential to the efficacy of combined 5AZA-C + DFMO treatment in an ovarian cancer mouse model. **A,** Treatment schematic for dosing with macrophage block antibody α-CSF1R. All mice were drained during each ascites draining procedure beginning at week 7. **B,** Reduction in total macrophages observed at the first drain (week 7 on schematic). **C,** ELISA of M-CSF levels demonstrating an increase in circulating M-CSF in the presence of receptor block CSF1R. **D,** Tumor burden represented by ascites volume in mice treated with 5AZA-C + DFMO in presence of CSF1R antibody or IgG control during the second drain (week 8 on schematic in **A**). **E,** Tumor burden during the third drain (week 9 on schematic in **A**), demonstrating an increase in tumor burden in 5AZA-C + DFMO mice receiving CSF1R. **F,** Survival curve of 5AZA-C + DFMO–treated mice receiving CSF1R antibody. Mice with decreased macrophages due to the antibody demonstrated a decrease in survival compared with 5AZA-C + DFMO mice receiving IgG. **G,** M1 macrophages (MHC II$^+$ CD206$^-$) analyzed via flow cytometry. 5AZA-C + DFMO–treated mice receiving CSF1R showed no increase in M1 macrophages. **H,** M2 macrophages (MHC II$^-$ CD206$^+$) analyzed via flow cytometry. M2 macrophages were reduced in both 5AZA-C + DFMO treatment arms, compared with mock-treated mice. All data were tested for a Gaussian distribution and found to be normal using Shapiro–Wilk test. Significance was determined using a *t* test (**B** and **C**) or one-way ANOVA (**D, E, G,** and **H**). *, $P < 0.05$; **, $P < 0.01$; ***, $P < 0.001$; ****, $P < 0.0001$.

macrophages (23, 41). Inhibition of arginase I could lead to increased amounts of its substrate arginine, potentially providing more of the metabolite for use by M1 macrophages and iNOS (41, 49). Treatment with DFMO may therefore increase M1 macrophages by making more of its essential metabolite arginine available, whereas 5AZA-C may help increase M1 macrophages via its interferon response and production of IFNγ, a cytokine that drives M1 polarization (15, 18, 19, 49).

Depletion of macrophages in the tumor microenvironment using a CSF1R antibody significantly diminished the efficacy of combination 5AZA-C and DFMO, and decreased the levels of M1 macrophages. Tumor burden recurred more rapidly and survival was diminished in mice with fewer macrophages, suggesting that these M1 macrophages could have a tumoricidal role in ovarian tumors. This work represents the first combination of these two distinct treatment strategies in any cancer. The impact of 5AZA-C and DFMO on macrophages in the tumor microenvironment may not be specific to ovarian cancer, and could therefore possibly translate to other macrophage-rich tumors. Furthermore, the use of two well-tolerated and clinically approved drugs offers potential to test a third drug in combination to further prolong survival. Exploration of additional drugs that potentiate M1 macrophages is important, as these tumoricidal cells have potential to decrease tumor burden and help activate the immune system against cancer.

Disclosure of Potential Conflicts of Interest

K.E. Bachman has ownership interest (including stock, patents, etc.) in Johnson & Johnson. C.A. Zahnow reports receiving Commercial Research Grant from Janssen Pharmaceuticals Inc. No conflicts of interest were disclosed by the other authors.

Authors' Contributions

Conception and design: M. Travers, S.M. Brown, K.E. Bachman, S.B. Baylin, R.A. Casero, Jr., C.A. Zahnow
Development of methodology: M. Travers, S.M. Brown, R.A. Casero, Jr., C.A. Zahnow
Acquisition of data (provided animals, acquired and managed patients, provided facilities, etc.): M. Travers, S.M. Brown, M. Dunworth, C.E. Holbert, K.R. Wiehagen, J.R. Foley, M.L. Stone
Analysis and interpretation of data (e.g., statistical analysis, biostatistics, computational analysis): M. Travers, S.M. Brown, M. Dunworth, K.R. Wiehagen, R.A. Casero, Jr., C.A. Zahnow
Writing, review, and/or revision of the manuscript: M. Travers, C.E. Holbert, K.E. Bachman, S.B. Baylin, R.A. Casero, Jr., C.A. Zahnow
Administrative, technical, or material support (i.e., reporting or organizing data, constructing databases): M. Travers, S.M. Brown, K.R. Wiehagen
Study supervision: K.E. Bachman, R.A. Casero, Jr., C.A. Zahnow

Acknowledgments

This work was supported by the NCI under award number R01CA204345 (to R.A. Casero, Jr.) and P30CA006973 (SKCCC Core Grant). The content is solely the responsibility of the authors and does not represent official views of the NIH. This work was also supported in part by Janssen, the SWCRF Collaboration for a Cure Grant, the Irving A. Hansen Memorial Foundation, and the Dr. Miriam and Sheldon G. Adelson Medical Research Foundation.

The costs of publication of this article were defrayed in part by the payment of page charges. This article must therefore be hereby marked *advertisement* in accordance with 18 U.S.C. Section 1734 solely to indicate this fact.

Received December 20, 2018; revised March 25, 2019; accepted May 7, 2019; published first May 14, 2019.

References

1. Siegel RL, Miller KD, Jemal A. Cancer statistics, 2018. CA Cancer J Clin 2018;68:7–30.
2. Alipour S, Zoghi S, Khalili N, Hirbod-Mobarakeh A, Emens LA, Rezaei N. Specific immunotherapy in ovarian cancer: a systematic review. Immunotherapy 2016;8:1193–204.
3. Chester C, Dorigo O, Berek JS, Kohrt H. Immunotherapeutic approaches to ovarian cancer treatment. J Immunother Cancer 2015;3:7.
4. Preston CC, Goode EL, Hartmann LC, Kalli KR, Knutson KL. Immunity and immune suppression in human ovarian cancer. Immunotherapy 2011;3:539–56.
5. Brahmer JR, Tykodi SS, Chow LQ, Hwu WJ, Topalian SL, Hwu P, et al. Safety and activity of anti-PD-L1 antibody in patients with advanced cancer. N Engl J Med 2012;366:2455–65.
6. Leffers N, Gooden MJ, de Jong RA, Hoogeboom BN, ten Hoor KA, Hollema H, et al. Prognostic significance of tumor-infiltrating T-lymphocytes in primary and metastatic lesions of advanced stage ovarian cancer. Cancer Immunol Immunother 2009;58:449–59.
7. Wu L, Deng Z, Peng Y, Han L, Liu J, Wang L, et al. Ascites-derived IL-6 and IL-10 synergistically expand CD14(+)HLA-DR(-/low) myeloid-derived suppressor cells in ovarian cancer patients. Oncotarget 2017;8:76843–56.
8. Zhang M, He Y, Sun X, Li Q, Wang W, Zhao A, et al. A high M1/M2 ratio of tumor-associated macrophages is associated with extended survival in ovarian cancer patients. J Ovarian Res 2014;7:19.
9. Yuan X, Zhang J, Li D, Mao Y, Mo F, Du W, et al. Prognostic significance of tumor-associated macrophages in ovarian cancer: a meta-analysis. Gynecol Oncol 2017;147:181–7.
10. Galli SJ, Borregaard N, Wynn TA. Phenotypic and functional plasticity of cells of innate immunity: macrophages, mast cells and neutrophils. Nat Immunol 2011;12:1035–44.
11. Bingle L, Brown NJ, Lewis CE. The role of tumour-associated macrophages in tumour progression: implications for new anticancer therapies. J Pathol 2002;196:254–65.
12. Tamura R, Tanaka T, Yamamoto Y, Akasaki Y, Sasaki H. Dual role of macrophage in tumor immunity. Immunotherapy 2018;10:899–909.
13. Wrangle J, Wang W, Koch A, Easwaran H, Mohammad HP, Vendetti F, et al. Alterations of immune response of non-small cell lung cancer with azacytidine. Oncotarget 2013;4:2067–79.
14. Li H, Chiappinelli KB, Guzzetta AA, Easwaran H, Yen RW, Vatapalli R, et al. Immune regulation by low doses of the DNA methyltransferase inhibitor 5-azacitidine in common human epithelial cancers. Oncotarget 2014;5:587–98.
15. Chiappinelli KB, Strissel PL, Desrichard A, Li H, Henke C, Akman B, et al. Inhibiting DNA methylation causes an interferon response in cancer via dsRNA including endogenous retroviruses. Cell 2015;162:974–86.
16. Roulois D, Loo Yau H, Singhania R, Wang Y, Danesh A, Shen SY, et al. DNA-Demethylating agents target colorectal cancer cells by inducing viral mimicry by endogenous transcripts. Cell 2015;162:961–73.
17. Wang L, Amoozgar Z, Huang J, Saleh MH, Xing D, Orsulic S, et al. Decitabine enhances lymphocyte migration and function and synergizes with CTLA-4 blockade in a murine ovarian cancer model. Cancer Immunol Res 2015;3:1030–41.
18. Stone ML, Chiappinelli KB, Li H, Murphy LM, Travers ME, Topper MJ, et al. Epigenetic therapy activates type I interferon signaling in murine ovarian cancer to reduce immunosuppression and tumor burden. Proc Natl Acad Sci U S A 2017;114:E10981–E90.
19. Topper MJ, Vaz M, Chiappinelli KB, DeStefano Shields CE, Niknafs N, Yen RC, et al. Epigenetic therapy Ties MYC depletion to reversing immune evasion and treating lung cancer. Cell 2017;171:1284–300.e21.
20. Tsai HC, Li H, Van Neste L, Cai Y, Robert C, Rassool FV, et al. Transient low doses of DNA-demethylating agents exert durable antitumor effects on hematological and epithelial tumor cells. Cancer Cell 2012;21:430–46.
21. Juergens RA, Wrangle J, Vendetti FP, Murphy SC, Zhao M, Coleman B, et al. Combination epigenetic therapy has efficacy in patients with refractory advanced non-small cell lung cancer. Cancer Discov 2011;1:598–607.
22. Hayes CS, Shicora AC, Keough MP, Snook AE, Burns MR, Gilmour SK. Polyamine-blocking therapy reverses immunosuppression in the tumor microenvironment. Cancer Immunol Res 2014;2:274–85.
23. Casero RA Jr., Murray Stewart T, Pegg AE. Polyamine metabolism and cancer: treatments, challenges and opportunities. Nat Rev Cancer 2018:18:681–95.
24. Pegg AE.Regulation of ornithine decarboxylase. J Biol Chem 2006;281:14529–32.
25. Abeloff MD, Rosen ST, Luk GD, Baylin SB, Zeltzman M, Sjoerdsma A. Phase II trials of alpha-difluoromethylornithine, an inhibitor of polyamine synthesis, in advanced small cell lung cancer and colon cancer. Cancer Treat Rep 1986;70:843–5.
26. Abeloff MD, Slavik M, Luk GD, Griffin CA, Hermann J, Blanc O, et al. Phase I trial and pharmacokinetic studies of alpha-difluoromethylornithine—an inhibitor of polyamine biosynthesis. J Clin Oncol 1984;2:124–30.
27. Bassiri H, Benavides A, Haber M, Gilmour SK, Norris MD, Hogarty MD. Translational development of difluoromethylornithine (DFMO) for the treatment of neuroblastoma. Transl Pediatr 2015;4:226–38.
28. Heby O, Persson L, Rentala M. Targeting the polyamine biosynthetic enzymes: a promising approach to therapy of African sleeping sickness, Chagas' disease, and leishmaniasis. Amino Acids 2007;33:359–66.
29. Kansiime F, Adibaku S, Wamboga C, Idi F, Kato CD, Yamuah L, et al. A multicentre, randomised, non-inferiority clinical trial comparing a nifurtimox-eflornithine combination to standard eflornithine monotherapy for late stage Trypanosoma brucei gambiense human African trypanosomiasis in Uganda. Parasit Vectors 2018;11:105.
30. Laukaitis CM, Gerner EW. DFMO: targeted risk reduction therapy for colorectal neoplasia. Best Pract Res Clin Gastroenterol 2011;25:495–506.
31. Meyskens FL Jr., McLaren CE, Pelot D, Fujikawa-Brooks S, Carpenter PM, Hawk E, et al. Difluoromethylornithine plus sulindac for the prevention of

sporadic colorectal adenomas: a randomized placebo-controlled, double-blind trial. Cancer Prev Res (Phila) 2008;1:32–8.
32. Zell JA, Pelot D, Chen WP, McLaren CE, Gerner EW, Meyskens FL. Risk of cardiovascular events in a randomized placebo-controlled, double-blind trial of difluoromethylornithine plus sulindac for the prevention of sporadic colorectal adenomas. Cancer Prev Res (Phila) 2009;2:209–12.
33. Ye C, Geng Z, Dominguez D, Chen S, Fan J, Qin L, et al. Targeting ornithine decarboxylase by alpha-difluoromethylornithine inhibits tumor growth by impairing myeloid-derived suppressor cells. J Immunol 2016;196:915–23.
34. Roby KF, Taylor CC, Sweetwood JP, Cheng Y, Pace JL, Tawfik O, et al. Development of a syngeneic mouse model for events related to ovarian cancer. Carcinogenesis 2000;21:585–91.
35. Conejo-Garcia JR, Benencia F, Courreges MC, Kang E, Mohamed-Hadley A, Buckanovich RJ, et al. Tumor-infiltrating dendritic cell precursors recruited by a beta-defensin contribute to vasculogenesis under the influence of Vegf-A. Nat Med 2004;10:950–8.
36. Kabra PM, Lee HK, Lubich WP, Marton LJ. Solid-phase extraction and determination of dansyl derivatives of unconjugated and acetylated polyamines by reversed-phase liquid chromatography: improved separation systems for polyamines in cerebrospinal fluid, urine and tissue. J Chromatogr 1986;380:19–32.
37. Peirce CS.The numerical measure of the success of predictions. Science 1884;4:453–4.
38. Duraiswamy J, Freeman GJ, Coukos G. Therapeutic PD-1 pathway blockade augments with other modalities of immunotherapy T-cell function to prevent immune decline in ovarian cancer. Cancer Res 2013;73:6900–12.
39. Wherry EJ, Kurachi M. Molecular and cellular insights into T cell exhaustion. Nat Rev Immunol 2015;15:486–99.
40. Zehn D, Wherry EJ. Immune memory and exhaustion: clinically relevant lessons from the LCMV model. Adv Exp Med Biol 2015;850:137–52.
41. Bronte V, Zanovello P.Regulation of immune responses by L-arginine metabolism. Nat Rev Immunol 2005;5:641–54.
42. Lawrence T, Natoli G.Transcriptional regulation of macrophage polarization: enabling diversity with identity. Nat Rev Immunol 2011;11:750–61.
43. Sica A, Mantovani A. Macrophage plasticity and polarization: in vivo veritas. J Clin Invest 2012;122:787–95.
44. Martinez FO, Gordon S.The M1 and M2 paradigm of macrophage activation: time for reassessment. F1000Prime Rep 2014;6:13.
45. MacDonald KP, Palmer JS, Cronau S, Seppanen E, Olver S, Raffelt NC, et al. An antibody against the colony-stimulating factor 1 receptor depletes the resident subset of monocytes and tissue- and tumor-associated macrophages but does not inhibit inflammation. Blood 2010;116:3955–63.
46. Manetta A, Satyaswarcoop PG, Podczaski ES, Hamilton T, Ozols RF, Mortel R. Effect of alpha-difluoromethylornithine (DFMO) on the growth of human ovarian carcinoma. Eur J Gynaecol Oncol 1988;9:222–7.
47. Peng M, Yin N, Chhangawala S, Xu K, Leslie CS, Li MO. Aerobic glycolysis promotes T helper 1 cell differentiation through an epigenetic mechanism. Science 2016;354:481–4.
48. Baydoun AR, Morgan DM.Inhibition of ornithine decarboxylase potentiates nitric oxide production in LPS-activated J774 cells. Br J Pharmacol 1998;125:1511–6.
49. Mantovani A, Marchesi F, Malesci A, Laghi L, Allavena P. Tumour-associated macrophages as treatment targets in oncology. Nat Rev Clin Oncol 2017;14:399–416.